Article

Molecular Cell

The DNA Damage Checkpoint Eliminates Mouse Oocytes with Chromosome Synapsis Failure

Graphical Abstract

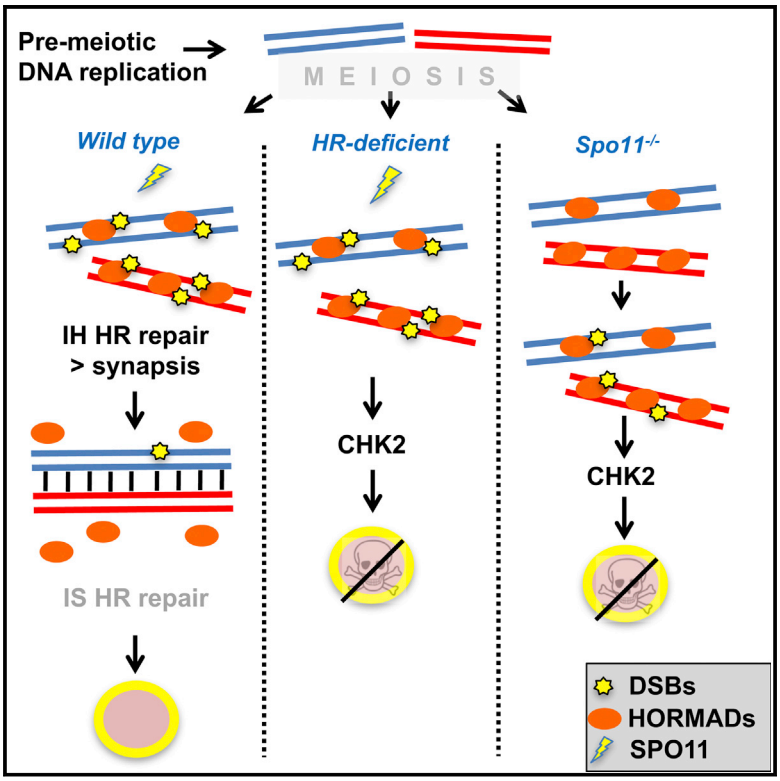

Highlights

- Late meiosis I oocytes bearing more than 10 DSBs are killed by the DNA damage checkpoint
- CHK2 is responsible for eliminating many asynaptic, SPO11-deficient mouse oocytes
- *Spo11*$^{-/-}$ oocytes acquire spontaneous DSBs that often exceed the 10-DSB threshold
- HORMAD2 on pachytene chromosomes prevents DSB repair via intersister recombination

Authors

Vera D. Rinaldi, Ewelina Bolcun-Filas, Hiroshi Kogo, Hiroki Kurahashi, John C. Schimenti

Correspondence

jcs92@cornell.edu

In Brief

Proper chromosome segregation during meiosis requires recombination repair of programmed DNA breaks to drive homolog pairing. Gametes with potentially devastating unsynapsed chromosomes or unrepaired breaks are killed. Surprisingly, Rinaldi et al. find that the CHK2 DNA damage checkpoint is important for eliminating mutant oocytes with either type of defect.

Rinaldi et al., 2017, Molecular Cell 67, 1026–1036
September 21, 2017
http://dx.doi.org/10.1016/j.molcel.2017.07.027

CellPress

Molecular Cell
Article

The DNA Damage Checkpoint Eliminates Mouse Oocytes with Chromosome Synapsis Failure

Vera D. Rinaldi,[1] Ewelina Bolcun-Filas,[1,2] Hiroshi Kogo,[4] Hiroki Kurahashi,[3] and John C. Schimenti[1,5,*]
[1]Cornell University, Departments of Biomedical Sciences and Molecular Biology and Genetics, Ithaca, NY 14850, USA
[2]The Jackson Laboratory, Bar Harbor, ME 14850, USA
[3]Fujita Health University, Institute of Comprehensive Molecular Science, Toyoake, Aichi 470-1192, Japan
[4]Gunma University, Department of Anatomy and Cell Biology, Maebashi, Gunma 371-8511, Japan
[5]Lead Contact
*Correspondence: jcs92@cornell.edu
http://dx.doi.org/10.1016/j.molcel.2017.07.027

SUMMARY

Pairing and synapsis of homologous chromosomes during meiosis is crucial for producing genetically normal gametes and is dependent upon repair of SPO11-induced double-strand breaks (DSBs) by homologous recombination. To prevent transmission of genetic defects, diverse organisms have evolved mechanisms to eliminate meiocytes containing unrepaired DSBs or unsynapsed chromosomes. Here we show that the CHK2 (CHEK2)-dependent DNA damage checkpoint culls not only recombination-defective mouse oocytes but also SPO11-deficient oocytes that are severely defective in homolog synapsis. The checkpoint is triggered in oocytes that accumulate a threshold level of spontaneous DSBs (~10) in late prophase I, the repair of which is inhibited by the presence of HORMAD1/2 on unsynapsed chromosome axes. Furthermore, *Hormad2* deletion rescued the fertility of oocytes containing a synapsis-proficient, DSB repair-defective mutation in a gene (*Trip13*) required for removal of HORMADs from synapsed chromosomes, suggesting that many meiotic DSBs are normally repaired by intersister recombination in mice.

INTRODUCTION

Genome maintenance in germ cells is critical for fertility, prevention of birth defects, and the genetic stability of species. Throughout mammalian germline development, from primordial germ cells (PGCs) through completion of meiosis, there are mechanisms that prevent the transmission of gametes with genetic defects. Indeed, mutation rates in germ cells are far lower than in somatic cells (Conrad et al., 2011; Murphey et al., 2013; Stambrook and Tichy, 2010). This is reflected by the exquisite sensitivity of PGCs to mutations in certain DNA repair genes (Agoulnik et al., 2002; Luo et al., 2014; Nadler and Braun, 2000) (Watanabe et al., 2013), sensitivity of resting oocytes to clastogens such as radiation and chemotherapeutics (Maltaris et al., 2007; Perez et al., 1997; Suh et al., 2006), and sensitivity of developing prophase I meiocytes to genetic anomalies, including a modicum of DNA damage (Meirow and Nugent, 2001; Suh et al., 2006) or the presence of a single asynapsed chromosome or even a chromosomal subregion (Burgoyne and Baker, 1985; Homolka et al., 2012).

Genetic and developmental analyses of mouse mutants have suggested that there are at least two distinct checkpoints during meiotic prophase I in oocytes, one that monitors double-strand break (DSB) repair and another that monitors synapsis. Oocytes defective for either synapsis or DSB repair are eliminated with different dynamics and severity. Females with mutations causing pervasive asynapsis alone (e.g., *Spo11*$^{-/-}$) are born with a grossly reduced oocyte pool. The surviving oocytes undergo folliculogenesis but are reproductively inviable, becoming exhausted within a few weeks by atresia and ovulation (Di Giacomo et al., 2005). Oocytes defective in DSB repair alone (*Trip13*$^{Gt/Gt}$) or defective in both synapsis and meiotic DSB repair (e.g., *Dmc1*$^{-/-}$; *Msh5*$^{-/-}$) are virtually completely eliminated between late gestation and wean age by the action of a DNA damage checkpoint (Di Giacomo et al., 2005; Li and Schimenti, 2007). Furthermore, genetic ablation of meiotic DSB formation confers a *Spo11*$^{-/-}$-like phenotype to such DSB repair mutants, consistent with the existence of separate DNA damage and synapsis checkpoints (Di Giacomo et al., 2005; Finsterbusch et al., 2016; Li and Schimenti, 2007; Reinholdt and Schimenti, 2005). For DSB repair, CHK2 (checkpoint kinase 2) signaling to TRP53/TAp63 is crucial for eliminating *Trip13*$^{Gt/Gt}$ mutant oocytes that exhibit full chromosome synapsis but have unrepaired SPO11-induced DSBs (Bolcun-Filas et al., 2014). Interestingly, *Chk2* deficiency imparted a *Spo11* null-like phenotype upon *Dmc1*$^{-/-}$ ovaries, consistent with separate, sequentially acting checkpoints (Bolcun-Filas et al., 2014). Genetic evidence for a distinct synapsis checkpoint came from studies of mice lacking HORMAD1 or HORMAD2, proteins that load onto axes of meiotic chromosomes throughout early prophase I but are removed upon synapsis (Wojtasz et al., 2009). Ablation of either in mice prevented loss of SPO11-deficient oocytes, resulting in the persistence of a nonfertile primordial follicle reserve in adults (Daniel et al., 2011; Kogo et al., 2012a; Wojtasz et al., 2012). These data suggest that the HORMADs are components of a synapsis checkpoint pathway. Another mechanism for elimination of oocytes is related to the phenomenon of MSUC (meiotic

silencing of unsynapsed chromatin). Although not formally a checkpoint, the transcriptional inactivation of a chromosome containing genes essential for oocyte survival and development can block progression past diplonema (Cloutier et al., 2015).

Although these lines of evidence support the existence of separate checkpoints monitoring DNA damage and synapsis, studies in non-mammalian organisms indicate that the "pachytene checkpoint"—a term referring to delayed progression of meiosis or death of meiocytes triggered by genetic aberrations present in late pachynema—is more complex, consisting of both distinct and overlapping signaling pathways that also affect DNA repair modalities such as choice of recombination partner for the repair of meiotic DSBs (e.g., sister chromatid versus homolog) (Joshi et al., 2015; MacQueen and Hochwagen, 2011; Roeder and Bailis, 2000; Subramanian and Hochwagen, 2014). Here we report the results of a series of experiments designed to discriminate whether the pachytene checkpoint in mouse oocytes indeed consists of distinct pathways responding to different signals or whether the responses are integrated into a single checkpoint pathway. Using a variety of mouse mutants, we show that most oocytes that are highly defective for chromosome synapsis accumulate spontaneous DSBs at a level that can trigger the CHK2-dependent DNA damage signaling pathway, leading to their elimination. Additionally, we present evidence that the reason why asynaptic *Spo11*$^{-/-}$ oocytes can be rescued by HORMAD1/2 deficiency is that their absence disrupts the so-called barrier to sister chromatid recombination (BSCR), enabling intersister (IS) repair of those spontaneous DSBs. Taken together, we propose that the pachytene checkpoint consists primarily of a canonical DNA damage signaling pathway and that extensive asynapsis leads to oocyte loss by inhibiting homologous recombination (HR) repair rather than triggering a distinct "synapsis checkpoint."

RESULTS

CHK2 Is Involved in the Elimination of *Spo11*$^{-/-}$ Oocytes

To investigate potential overlap of the meiotic DSB repair and synapsis checkpoint pathways in mice, we tested whether CHK2, a well-defined DSB signal transducer, contributes to the elimination of *Spo11*$^{-/-}$ oocytes that are asynaptic because of lack of programmed meiotic DSBs needed for recombination-driven homolog pairing. Consistent with prior reports (Baudat et al., 2000; Di Giacomo et al., 2005), we observed a greatly reduced number of total follicles in 3-week-postpartum (pp) *Spo11*$^{-/-}$ ovaries compared with the WT, and, in particular, the oocyte reserve (the pool of primordial resting follicles) was almost completely exhausted by 8 weeks of age (Figure 1). Surprisingly, *Chk2* deletion rescued the oocyte reserve (Figures 1A and 1B), albeit not to WT levels. The rescued follicles in double-mutant females persisted robustly at least until 6 months pp (in one case, 554 total in a single ovary).

HORMAD2 Deficiency Prevents Elimination of *Trip13* Mutant Oocytes that Have Complete Synapsis but Unrepaired Meiotic DSBs, Restoring Female Fertility

Taken alone, the rescue of *Spo11*$^{-/-}$ oocytes by *Chk2* deletion suggests that severe asynapsis leads to CHK2 activation and signaling to mediate oocyte elimination. This led us to postulate that either CHK2 is a common component of otherwise distinct synapsis and DNA damage checkpoints or that there is a single linear checkpoint pathway that responds to both asynapsis and DNA damage and that DNA damage activates the checkpoint pathway more robustly or sooner in prophase I (thus accounting for the different patterns of oocyte elimination in asynaptic versus DSB repair-deficient oocytes mentioned above; Di Giacomo et al., 2005).

We reasoned that if there is a single linear checkpoint pathway, then putative synapsis checkpoint genes required to eliminate *Spo11*$^{-/-}$ oocytes would also be required to eliminate *Trip13*$^{Gt/Gt}$ oocytes. *Trip13*$^{Gt/Gt}$ meiocytes have synapsed chromosomes and persistent SPO11-dependent DSBs, which leads to neonatal depletion of follicles in a CHK2 > TRP53/TAp63 pathway-dependent manner (Figure 2A; Bolcun-Filas et al., 2014; Li and Schimenti, 2007). To test this, we determined whether deficiency of HORMAD2, a putative synapsis checkpoint protein, could rescue *Trip13*$^{Gt/Gt}$ oocytes. HORMAD2 and its paralog HORMAD1 are HORMA (Hop1, Rev7, and Mad2) domain-containing proteins orthologous to the *Saccharomyces cerevisiae* synaptonemal complex (SC) axial element protein Hop1p, and deletion of either prevents elimination of *Spo11*$^{-/-}$ oocytes (Daniel et al., 2011; Kogo et al., 2012a; Wojtasz et al., 2012). We used a mutant of *Hormad2* rather than *Hormad1* because deletion of the latter disrupts recombination and homolog synapsis (Daniel et al., 2011; Kogo et al., 2012b; Shin et al., 2010). Remarkably, not only did ovaries of 2-month-old *Trip13*$^{Gt/Gt}$ *Hormad2*$^{-/-}$ mice retain a substantial primordial follicle pool (Figures 2A and 2B), but these females were also fertile (Figure 2C). The rescued fertility of these oocytes suggests either that these DSBs were compatible with further oocyte maturation or that they were eventually repaired, as in the case of *Trip13*$^{Gt/Gt}$ females, whose fertility was restored by *Chk2* ablation (Bolcun-Filas et al., 2014). The dynamics of DSB repair are addressed below.

Because TRIP13 is required for removal of the HORMADs from chromosome axes upon synapsis (Wojtasz et al., 2009), and persistence of HORMADs on unsynapsed chromosomes correlates with MSUC-mediated silencing of essential genes (Cloutier et al., 2015; Wojtasz et al., 2012), the question arises of whether *Trip13*$^{Gt/Gt}$ oocytes are eliminated not because of unrepaired DSBs but, rather, by transcriptional silencing. However, this is unlikely for the following reasons. First, *Trip13*$^{Gt/Gt}$ oocytes are depleted with a temporal pattern and degree consistent with mutants defective in DSB repair, not asynapsis (Di Giacomo et al., 2005; Li and Schimenti, 2007). Second, *Spo11* is epistatic to *Trip13* in that *Trip13*$^{Gt/Gt}$ *Spo11*$^{-/-}$ ovaries resemble *Spo11* single mutants in their pattern of oocyte elimination (Li and Schimenti, 2007), demonstrating that unrepaired meiotic DSBs drive early culling of *Trip13* mutant oocytes. Third, HORMAD persistence on synapsed *Trip13*$^{Gt/Gt}$ or unsynapsed *Spo11*$^{-/-}$ meiotic chromosome axes is not affected by *Chk2* deletion (Figure S1), which might be predicted if CHK2 was rescuing either mutant class by disrupting the ability of HORMADs to signal asynapsis. The latter is further supported by the fact that CHK2 depletion does not interfere with MSCI (meiotic sex chromosome inactivation), which is mechanistically similar or identical to MSUC, in

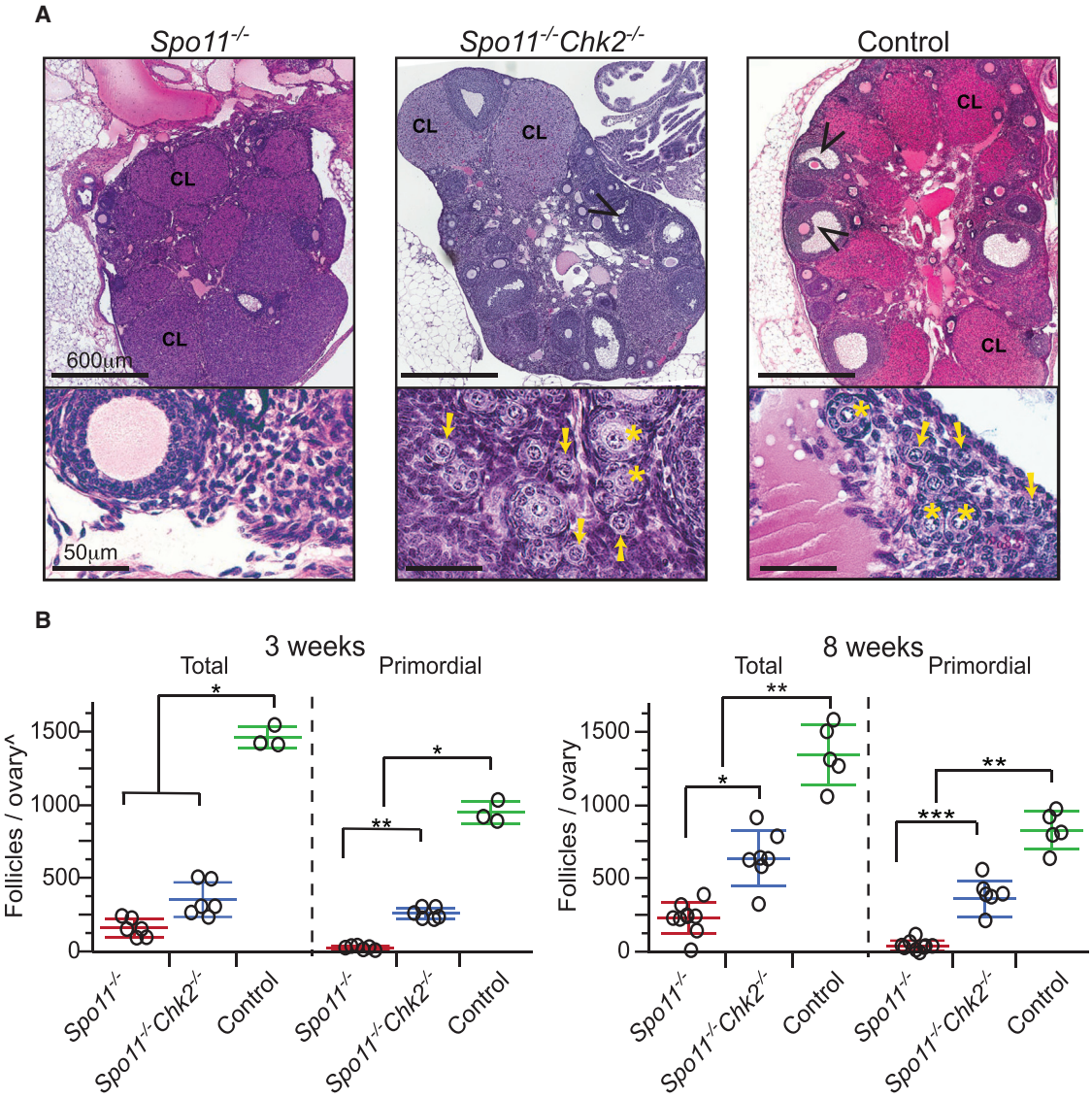

Figure 1. CHK2 Is Required for Efficient Elimination of Asynaptic *Spo11*$^{-/-}$ Mouse Oocytes

(A) H&E-stained histological sections of 8-week-old ovaries. Black arrowheads indicate antral follicles. The presence of corpora lutea (CL) is indicative of prior rounds of ovulation. Shown at the bottom are higher-magnification images of an ovarian cortical region, where primordial follicles reside. Yellow arrows and asterisks indicate primordial and primary follicles, respectively.

(B) Follicle counts from ovaries of the indicated genotypes at 3 and 8 weeks pp, respectively. Each data point is from a single ovary, each from a different animal. Total, all follicle types. Horizontal hashes denote mean and SD. Littermate controls included animals with the following genotypes: *Spo11*$^{+/+}$*Chk2*$^{+/+}$, *Spo11*$^{+/-}$ *Chk2*$^{+/-}$, and *Spo11*$^{+/+}$*Chk2*$^{+/-}$. ^, the values obtained for the 3-week follicles/ovaries counts are not comparable with the 8-week ones (see STAR Methods). *p = 0.005–0.05, **p = 0.001–0.005 and *** p $\leq$ 0.001 derived from a non-parametric, one-way ANOVA test (Kruskal-Wallis).

males (Pacheco et al., 2015) and that *Chk2*$^{-/-}$ mice are fertile, unlike *Hormad1*$^{-/-}$ animals (Daniel et al., 2011; Kogo et al., 2012b; Shin et al., 2013).

HORMAD2 Inhibits DSB Repair in Prophase I Oocytes

That HORMAD2 deficiency could rescue both *Trip13*$^{Gt/Gt}$ and *Spo11*$^{-/-}$ oocytes is consistent with a single checkpoint capable of detecting both damaged DNA and asynapsed chromosomes. If there is indeed a single checkpoint pathway, then combined deficiency for CHK2 and HORMAD2 should rescue asynaptic and DSB repair-defective *Dmc1*$^{-/-}$ oocytes to the same degree as deficiency for either one alone. However, *Dmc1*$^{-/-}$ *Chk2*$^{-/-}$ *Hormad2*$^{-/-}$ females had $\geq$3-fold increase in primordial and total follicles compared with *Dmc1*$^{-/-}$ *Hormad2*$^{-/-}$ or *Dmc1*$^{-/-}$ *Chk2*$^{-/-}$ ovaries (Figures 3A and 3B; Figure S2). This lack of epistasis indicates that HORMAD2 and CHK2 are not functioning solely as members of a single linear checkpoint pathway sensing either or both asynapsis and DNA damage.

We therefore considered two alternative explanations for why *Hormad2* deficiency rescues *Trip13*$^{Gt/Gt}$ oocytes: it reduces the

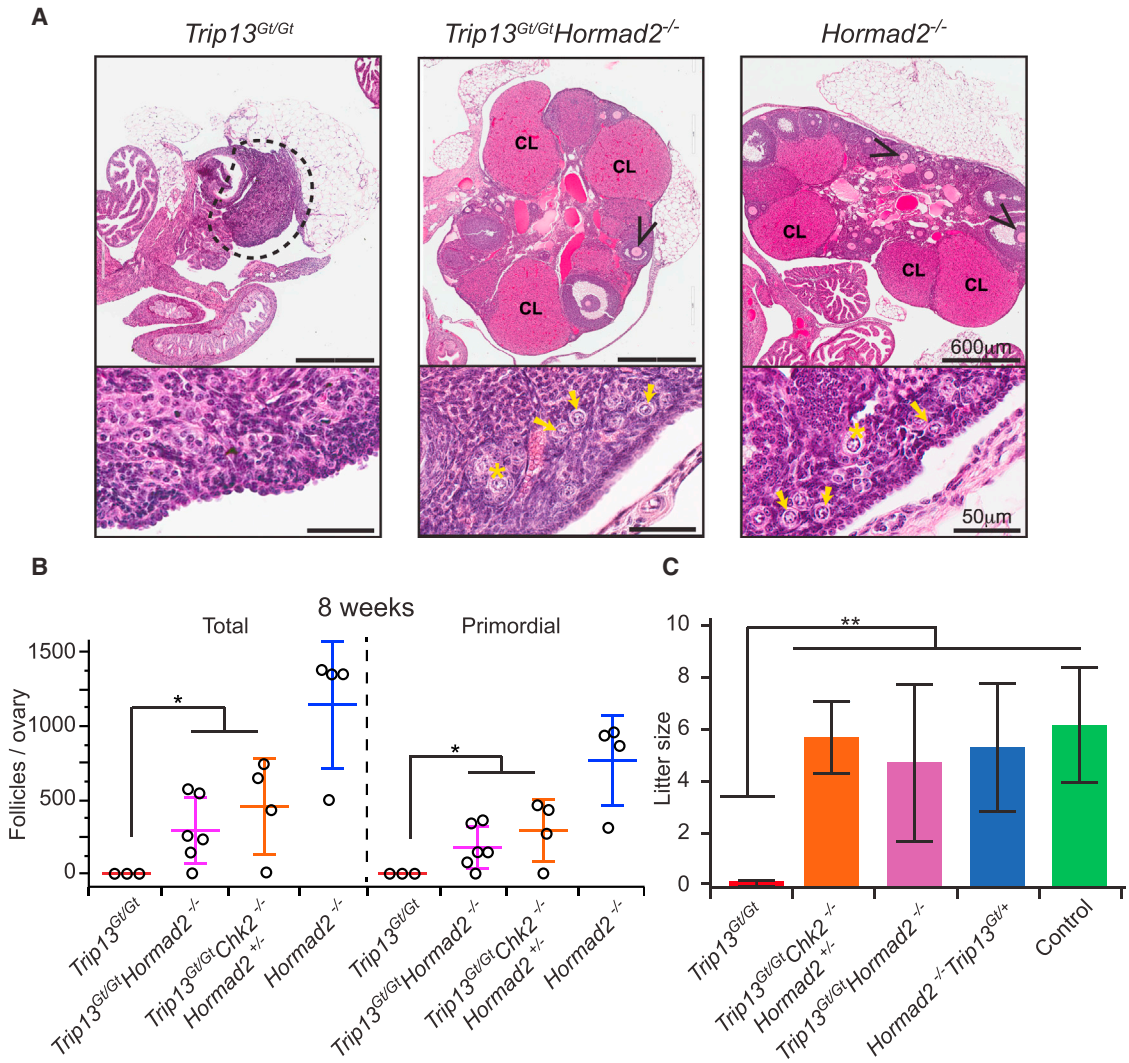

Figure 2. Synapsis-Competent *Trip13*$^{Gt/Gt}$ Oocytes Are Eliminated in a HORMAD2-Dependent Manner

(A) H&E-stained histological sections of 8-week-old ovaries of the indicated genotypes. Black arrowheads indicate antral follicles. Shown at the bottom are higher-magnification images of cortical regions of ovaries. Yellow arrows and asterisks indicate primordial and primary follicles, respectively.

(B) Follicle quantification of 8-week-old ovaries. Each data point is from a single ovary, each from a different animal. Total, all follicle types. Horizontal hashes denote mean and SD. The statistic used was a Kruskal-Wallis test. *p = 0.002.

(C) Graphed are mean litter sizes. n $\geq$ 3 females tested for fertility per genotypic group. Control matings were between mice with the genotypes *Trip13*$^{Gt/+}$ and *Trip13*$^{Gt/+}$ *Hormad2*$^{+/-}$. Error bars represent SD, and **p $\leq$ 0.005, derived from the Kruskal-Wallis test.

number of SPO11-induced DSBs to a level sufficient for synapsis but below the threshold for checkpoint activation, and/or it facilitates DSB repair. Studies of related proteins support both explanations. Absence of the budding yeast ortholog Hop1p not only decreases meiotic DSB formation but also increases use of the sister chromatid as a template for HR repair (Carballo et al., 2008; Lam and Keeney, 2014; Latypov et al., 2010; Mao-Draayer et al., 1996; Niu et al., 2005; Schwacha and Kleckner, 1997). Mouse HORMAD1 is required for loading HORMAD2 onto unsynapsed axes, proper SC formation (Daniel et al., 2011), and normal levels of meiotic DSBs (Daniel et al., 2011; Stanzione et al., 2016). Although *Dmc1*$^{-/-}$ *Hormad1*$^{-/-}$ or irradiated *Hormad1*$^{-/-}$ oocytes exhibit fewer DSB markers than oocytes containing HORMAD1 (Daniel et al., 2011; Shin et al., 2010), this can be attributable largely to enhanced repair (Shin et al., 2013). IS HR repair of DSBs in *S. cerevisiae* is substantial, and it increases in *hop1* mutants (Goldfarb and Lichten, 2010). Moreover, disruption of SC axes in mice (deletion of *Sycp2* or *Sycp3*) appears to alter recombination partner choice in favor of the sister chromatid, decreasing persistent DSBs in *Trip13*$^{Gt/Gt}$ oocytes to a degree that diminishes their elimination in a RAD54-dependent manner (Li et al., 2011). These data led us to hypothesize that the rescue of *Trip13* mutant oocytes by *Hormad2* deficiency was due to increased DSB repair, possibly by diminishing the BSCR.

To test this, we quantified the levels and rates of meiotic DSB repair in various genotypes of prophase I oocytes. Although the

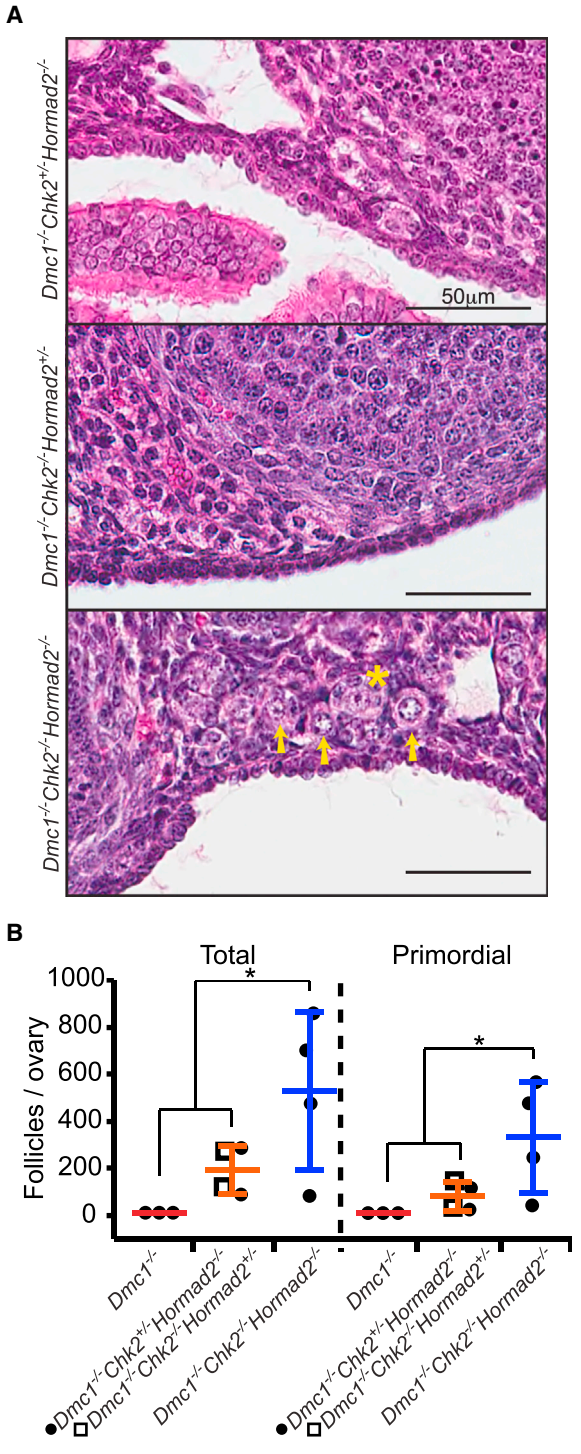

Figure 3. HORMAD2 and CHK2 Are Not in the Same Checkpoint Pathway

(A) H&E-stained histological sections of cortical regions of 8-week-old mutant mouse ovaries, where primordial follicles are concentrated. Histologies of whole ovaries of these genotypes are presented in Figure S2. Primordial follicles, which constitute the oocyte reserve, are indicated by yellow arrows, and a primary follicle by an asterisk. Residual *Dmc1*$^{-/-}$ ovaries are not represented because they are completely devoid of oocytes (Pittman et al., 1998).

(B) Follicle counts from ovaries of the indicated genotypes at 8 weeks of age. Total, all types of follicles. Data points represent follicle counts derived from one ovary, each ovary originating from a different animal. *p $\leq$ 0.05 (Kruskal-Wallis test).

number of leptotene- and zygotene-stage RAD51 foci was not significantly different in *Trip13*$^{Gt/Gt}$ *Hormad2*$^{-/-}$ oocytes compared with *Trip13*$^{Gt/Gt}$ or other control and mutant genotypes (Figures 4A and 4B; Table S1), there were significantly fewer compared with *Trip13*$^{Gt/Gt}$ by pachynema and diplonema ($p = 0.02$ and 0.03, respectively, using Tukey honest significant difference (HSD) in a mixed model). RAD51 levels in *Trip13*$^{Gt/Gt}$ and *Trip13*$^{Gt/Gt}$ *Chk2*$^{-/-}$ newborn oocytes remained high in diplonema compared with all other genotypes (Figures 4A and 4B; Table S1), presumably reflecting a relative deficiency in DSB repair. Furthermore, we found that RAD51 foci induced by 2 Gy of ionizing radiation (IR) disappeared more rapidly in *Spo11*$^{-/-}$ *Hormad2*$^{-/-}$ oocytes than in either *Spo11*$^{-/-}$ or *Spo11*$^{-/-}$ *Chk2*$^{-/-}$ oocytes, as assessed 8 hr after treatment (Figure 5; Table S2). Overall, the data suggest that HORMAD2 on the axes of either asynapsed (*Spo11*$^{-/-}$) or synapsed (*Trip13*$^{Gt/Gt}$) (Wojtasz et al., 2009) meiotic chromosomes inhibits IS recombination-mediated DSB repair.

Evidence that CHK2-Mediated Elimination of Asynaptic Oocytes Is Driven by Accumulation of SPO11-Independent DSBs

If indeed *Hormad2* deletion rescues DSB-containing oocytes by weakening or eliminating the BSCR, then this raises the question of why HORMAD2 deficiency rescues *Spo11*$^{-/-}$ oocytes that do not make meiotic DSBs. A clue comes from the surprising observation that *Spo11*$^{-/-}$ oocytes sustain DSBs of unknown origin (but possibly from LINE-1 retrotransposon activation) during early pachynema (Malki et al., 2014; Carofiglio et al., 2013). We hypothesized that these DSBs occur at levels sufficient to trigger the CHK2-dependent checkpoint in *Spo11*$^{-/-}$ oocytes but that, in the absence of SC axis-bound HORMAD2, there is sufficient DSB repair to prevent checkpoint activation. To test this, we determined the threshold number of DSBs that kills WT and *Chk2*$^{-/-}$ oocytes by exposing explanted newborn ovaries to a range of IR. RAD51 foci on chromosome axes accumulated roughly linearly in oocytes exposed to 0.5–9 Gy (Figure 6A; Figure S5), and *Chk2*$^{-/-}$ oocytes withstood up to 7 Gy (Figure 6B), a dosage that induces 73.3 RAD51 foci (Figure 6A). In contrast, as little as 0.3 Gy (10.3 foci by linear regression) abolished the entire primordial follicle pool of wild-type (WT) ovaries. Consistent with our hypothesis that HORMAD2 prevents DSB repair, the SC axes of *Spo11*$^{-/-}$ zygotene/pachytene-like chromosomes in newborn oocytes contained far more discrete RAD51 foci (raw average of 39.8; likely an underestimate; see Figure S3) than in *Spo11*$^{-/-}$ *Hormad2*$^{-/-}$ oocytes (average of 7.3 foci), the latter being almost identical to WT or *Chk2*$^{-/-}$ oocytes (7.5 and 7.3, respectively; Figure 6C; Table S3), in which HORMAD2 has been removed from synapsed chromosomes. These data indicate that the majority of *Spo11*$^{-/-}$ oocytes (60.8%) bear a level of DSBs (>10.3 foci) sufficient to trigger their elimination by the CHK2-dependent DNA damage checkpoint, whereas most WT oocytes (71%) are below this threshold (Table S3).

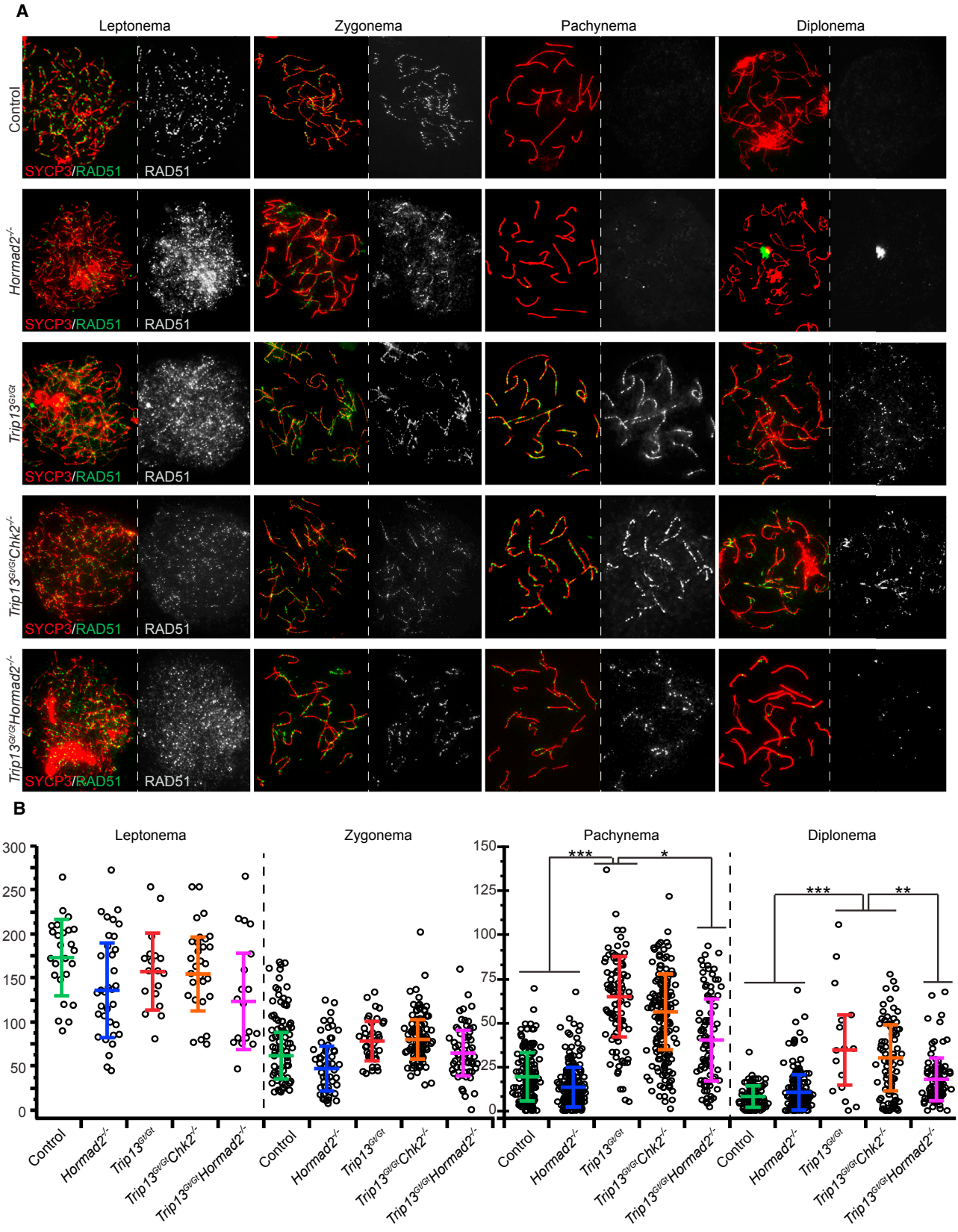

(legend on next page)

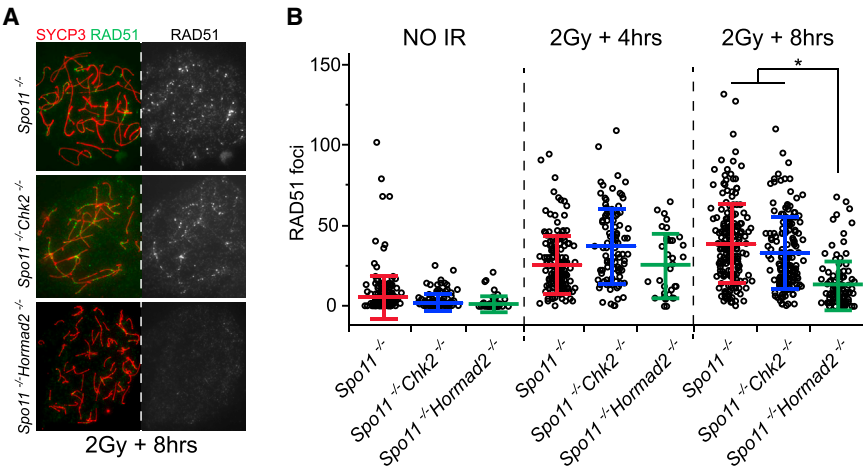

Figure 5. Depletion of HORMAD2 Accelerates Repair of Induced DSBs in Oocytes

(A) Immunolabeling of surface-spread chromosomes from oocytes after exposure to ionizing radiation (IR). Fetal ovaries were collected at 15.5 DPC, cultured for 24 hr, exposed to 2 Gy of IR, and then cultured for an additional 4-8 hr. Shown are those recovered 8 hr after IR. See Figure S4 for single *Hormad2*$^{-/-}$ single-mutant results.

(B) Quantification of RAD51 foci. Each data point represents one oocyte. The graphs include mean and SD and are color-coded according to genotypic group. The 4- and 8-hr unirradiated samples were combined. Data were derived from at least two different animals per condition. See Table S2 for associated raw data and statistical calculations.

DISCUSSION

Meiocytes have genetic quality control mechanisms that respond to their unique developmental circumstances, chromosome biology, and cell cycle. For example, the pachytene/prophase I checkpoint is active only at a point in prophase I at which DSBs have normally been repaired but not during the time between programmed DSB formation and HR repair. Although the oocyte pachytene checkpoint is distinct with respect to its cell cycle timing and its ability to monitor an event (chromosome synapsis) unique to meiosis, our current and prior (Bolcun-Filas et al., 2014) work indicate that, for circumstances involving extensive asynapsis and DNA damage, this checkpoint in oocytes involves a DNA damage response (DDR) common to somatic cells. Our surprising finding that the DDR is involved in culling of *Spo11*$^{-/-}$ oocytes raises the question of how SPO11-independent DSBs, first reported by Carofiglio et al. (2013) and confirmed here, arise on unsynapsed chromosomes. One possible source is LINE-1 retrotransposon activation, which has been correlated with natural oocyte attrition (Malki et al., 2014). However, transposon expression normally occurs only transiently at the onset of meiosis before epigenetic silencing (van der Heijden and Bortvin, 2009). It is possible that the extensive asynapsis in *Spo11*$^{-/-}$ oocytes per se or disruption of the meiotic program, including the normal course of DSB induction and repair, interferes with transposon silencing. Another possibility is that unsynapsed chromosomes are more susceptible to spontaneous breakage. These outcomes could be exacerbated by extended retention of HORMADs on unsynapsed axes, inhibiting repair of these breaks. An intriguing question is whether the production of these SPO11-independent DSBs, whatever their origin, evolved as a contributory mechanism for genetic quality control. It is also conceivable that the extended presence of HORMADs themselves contributes to spontaneous DSB formation, possibly as a "last ditch" mechanism to drive pairing or synapsis in chromosomes devoid of sufficient interhomolog recombination events.

The late appearance and highly variable number (Figure 6C) of SPO11-independent DSBs in *Spo11*$^{-/-}$ oocytes may explain the differences in timing and extent of oocyte elimination in exclusively asynaptic versus DSB repair-deficient (e.g., *Dmc1*, *Trip13*) mutants. As reported by Di Giacomo et al. (2005), although *Dmc1*$^{-/-}$ oocytes were completely eliminated before dictyate arrest and follicle formation, *Spo11*$^{-/-}$ ovaries contained ~15%–20% of the WT number of follicles (including 27-fold fewer primordial follicles by 4 days pp); this reduced oocyte reserve was depleted by 2–3 months of age by subsequent cycles of recruitment and maturation. Additionally, *Dmc1*$^{-/-}$ oocytes degenerate before *Spo11*$^{-/-}$ oocytes, suggesting that an earlier-acting mechanism was triggering *Dmc1*$^{-/-}$ oocyte death. These distinctions, in conjunction with epistasis analysis of mutants doubly deficient for *Spo11* and DSB repair mutations, led to the conclusion that there are DSB-dependent and -independent mechanisms to eliminate defective oocytes. We suggest that the difference in timing of oocyte elimination, at least in part, may be related to the DSB load. The abundant SPO11 DSBs formed early in prophase I may trigger the checkpoint sooner and more uniformly in recombination mutants that fail to reduce DSB levels in a timely manner. According to this scenario, spontaneous DSBs that do

Figure 4. Depletion of HORMAD2 Accelerates DSB Repair during Early Stages of Meiotic Prophase I

(A) Representative images of meiotic chromosome spreads from oocytes at different substages of meiotic prophase I, probed with antibodies for SYCP3 (SC axis protein) and the DSB marker RAD51. Oocytes were isolated from female embryos ranging from 15.5 DPC to newborns. See Figure S1 for HORMAD2 localization in meiotic mutants.

(B) Numbers of RAD51 foci in the specified meiotic prophase I substage of the indicated mutants. Only RAD51 foci present on SYCP3-stained axes were scored. Each data point represents one cell. In each genotypic group, at each stage, the counts are derived from at least three animals. Horizontal hashes in summary statistic plots denote mean and SD. Values of the mixed-model calculation can be found in Table S1. Colors correspond to genotypes. Asterisks indicate statistical significant differences between groups in terms of the least square means of RAD51 foci: ***p ≤ 0.001, **p ≤ 0.005, *p ≤ 0.05 (Tukey HSD). See Table S1 for associated raw data and statistical calculations.

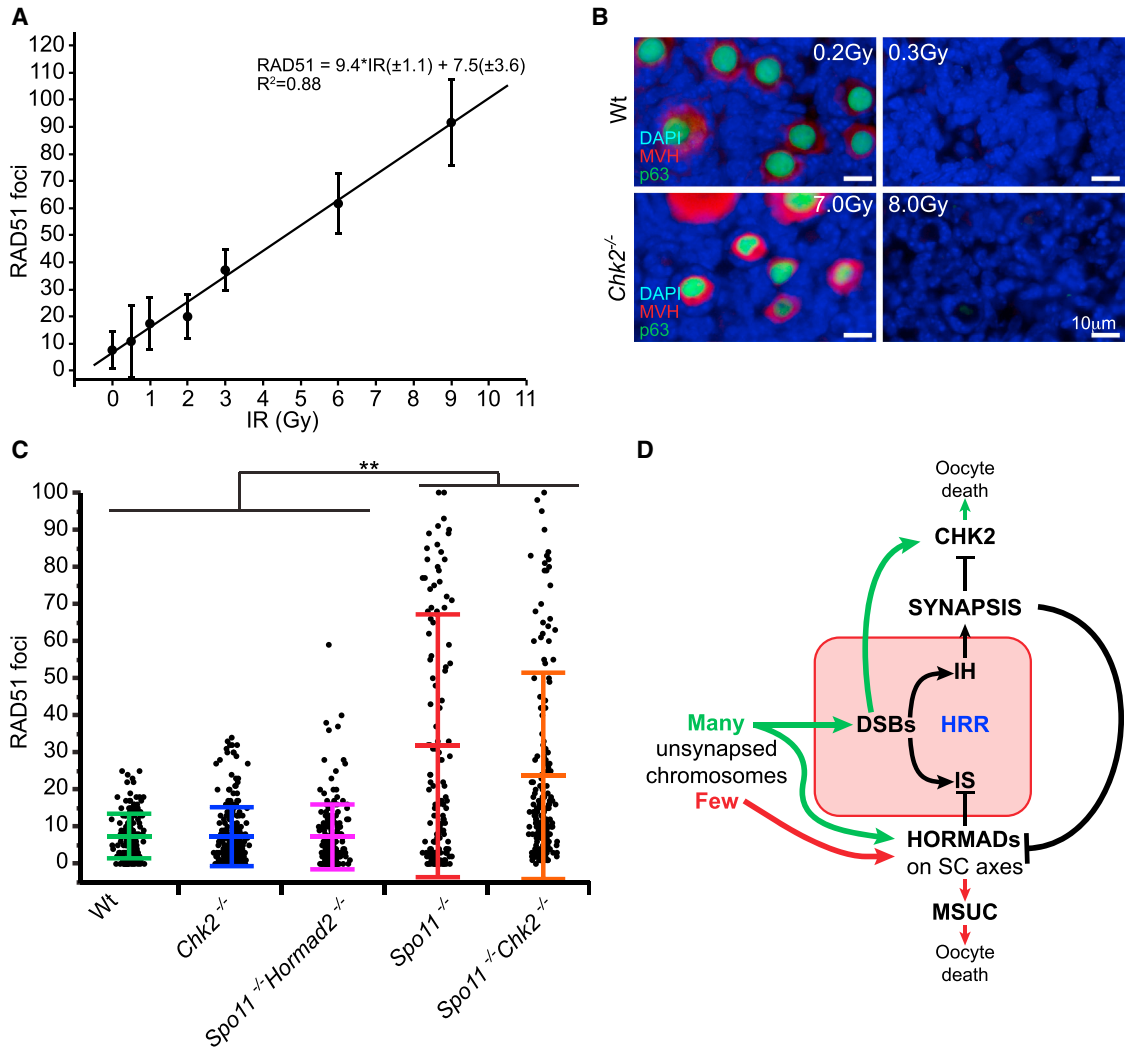

Figure 6. DNA Damage Threshold Required to Trigger Oocyte Death and Evidence for HORMAD-Mediated Inhibition of IS Repair

(A) Linear regression for conversion of radiation dosages to RAD51 focus counts. Meiotic surface spreads were made from WT neonatal ovaries 2.5 hr after IR. Plotted are means with SD. Each IR dose has focus counts from ~25 pachytene oocytes derived from a total of 18 animals. See Figure S5 for single-cell focus counts and numerical values.

(B) *Chk2*$^{-/-}$ oocytes are highly IR-resistant. Shown are immunofluorescence images of ovarian sections labeled with nuclear and cytoplasmic germ cell markers (p63 and MVH, respectively).

(C) RAD51 focus counts from newborn oocyte spreads. Only oocytes with discrete patterns of RAD51 foci were scored, as defined in Figure S3. Data points represent individual oocytes, derived from at least five different animals from each genotypic group. Horizontal hashes denote means and SD calculated using a mixed model (see STAR Methods). Asterisks indicate statistically significant differences between groups: ***p ≤ 0.001, **p ≤ 0.005, *p ≤ 0.05 (Tukey HSD). See Table S3 for raw data and statistical calculations.

(D) Model for pachytene checkpoint activation in mouse oocytes. Oocytes with many unsynapsed chromosomes (green) ultimately accumulate DSBs, which cannot be repaired because of block to IS recombination imposed by HORMADs on asynapsed axes. Failure of DSB repair leads to activation of CHK2 and downstream effector proteins (p53/TAp63) that trigger apoptosis. Few asynapsed chromosomes (red) lead to inactivation of essential genes by MSUC, thereby causing oocyte death.

not arise until latter stages of prophase I in *Spo11*$^{-/-}$ oocytes would trigger the DNA damage checkpoint at a later point. Based on our data (Figure 6A; Figure S5), we suggest that oocytes with below-threshold DSB levels escape the DNA damage checkpoint and are either eliminated by other mechanisms (see below) or survive to constitute the reduced follicular reserve in *Spo11* mutants.

Although the CHK2-dependent checkpoint is of central importance to genetic quality control in oocytes, our observations that *Chk2* deletion does not fully restore oocyte numbers to WT levels in mutants indicates that it is not absolutely required for eliminating all oocytes with unrepaired DSBs. Rather, the fraction of oocytes rescued is inversely related to the burden of unrepaired meiotic DSBs. For example, although *Chk2* deficiency rescued

nearly one-third of *Trip13*$^{Gt/Gt}$ oocytes (which are partially proficient for DSB repair and harbor 35 ± 4 and 63 ± 4.7 persistent RAD51 foci in diplonema and pachynema, respectively; Figure 4B), it rescued only a small fraction (~5%) of profoundly recombination-deficient *Dmc1*$^{-/-}$ oocytes (harboring an average of ~150 RAD51 foci; Li et al., 2011). We posit that the oocytes that fail to be rescued in these mutants are eliminated either by a separate or a complementary checkpoint pathway (for example, ATR-CHK1; Smith et al., 2010) or succumb to catastrophic levels of DNA damage. It is informative that deletion of *Hormad1*, but not *Hormad2*, rescues *Dmc1*$^{-/-}$ oocytes to a greater extent than *Chk2* deletion. As discussed earlier, the rescued *Dmc1*$^{-/-}$ *Hormad1*$^{-/-}$ oocytes had a marked reduction in DSBs (Bolcun-Filas et al., 2014; Shin et al., 2013; Wojtasz et al., 2012). Because HORMAD1 is needed to load HORMAD2 onto unsynapsed chromosome axes (not vice versa), the effect of *Hormad1* deletion upon IS recombination constitutes the combined roles of both HORMAD proteins. However, when *Hormad2* alone is deleted, the continued presence of chromosomally bound HORMAD1 may provide a less effective but still substantive BSCR. The lower level of residual DSBs in *Spo11* and *Trip13* mutant oocytes (compared with *Dmc1*$^{-/-}$) may render them responsive to a weaker BSCR, such as when *Hormad2* is deleted. We postulate that, because of its involvement in stimulating SPO11 activity (Daniel et al., 2011), *Hormad1* deletion is very effective in rescuing a DSB repair mutant like *Dmc1* because not only are fewer DSBs formed, but IS recombination is also more active.

Our results add to increasing evidence that IS recombination is important in mammalian meiosis. As discussed in the text, the HORMADs and SC axial element structure appear to inhibit IS repair of meiotic DSBs preferentially, thus allowing interhomolog (IH) recombination to drive homolog pairing and synapsis. However, as synapsis progresses and the SC is formed, the HORMADs are removed and, presumably, both IS and IH recombination can occur readily, as in yeast (Subramanian et al., 2016). Because not all RAD51 foci disappear by pachynema when synapsis is complete (for example, see Figure 4B), it is possible that a substantial fraction of these DSBs is normally repaired by IS recombination. We speculate that the persistent unrepaired DSBs on synapsed chromosomes of *Trip13* mutants, which retain HORMADs on their SCs, may actually constitute a substantial fraction of SPO11-induced DSBs (an average of ~65/oocyte nucleus of the 200–300 induced; Figure 4) that would normally be repaired by IS recombination. However, we cannot rule out the possibility that the "persistent" DSBs on synapsed *Trip13*$^{Gt/Gt}$ chromosomes actually arise from continued SPO11 cleavage signaled by continued presence of SC-bound HORMADs (Kauppi et al., 2013).

When trying to decipher the quality control mechanisms functioning during meiosis, it is important to recognize that experimental studies such as those performed here employ mutants with pervasive, non-physiological levels of defects. Meiocytes in WT individuals would have less extreme genetic defects. In oocytes bearing a small number (1–3) of unsynapsed chromosomes, the unsynapsed chromosomes undergo transcriptional silencing (MSUC) during pachynema, causing elimination at the diplotene stage (Cloutier et al., 2015; Kouznetsova et al., 2009) from lack of essential gene products encoded by these chromosomes (Cloutier et al., 2015). However, oocytes with more than 2–3 unsynapsed chromosomes impair MSUC, presumably because of a limiting amount of BRCA1 (Kouznetsova et al., 2009). Nevertheless, *Spo11*$^{-/-}$ meiocytes typically exhibit "pseudo sex bodies," named as such because they resemble the XY (sex) body involving a small number of asynapsed autosomes (Bellani et al., 2005). Formation of pseudo sex bodies in *Spo11*$^{-/-}$ oocytes is dependent on HORMADs (Daniel et al., 2011; Kogo et al., 2012b), leading to the proposal that these are responsible for oocyte elimination (Kogo et al., 2012a). This may be the case in a subset of oocytes where the pseudo sex body affects either a chromosomal region containing haploinsufficient loci or both alleles of a locus needed for meiotic progression or oocyte survival. Because CHK2 deficiency can rescue *Spo11*$^{-/-}$ oocytes while not abolishing HORMAD localization (Figure S1) or pseudo sex body formation (data not shown) but does not rescue all *Spo11* oocytes, it is likely that neither MSUC nor CHK2 alone is entirely responsible for elimination of all oocytes with pervasive asynapsis. Finally, because MSUC involves many components of the DNA damage response (Fernandez-Capetillo et al., 2003; Ichijima et al., 2011; Turner et al., 2004), it is conceivable that asynapsis leading to MSUC would activate effector elements of the DNA damage checkpoint pathway, including CHK2. However, this does not appear to be the case because silenced supernumerary chromosomes do not eliminate oocytes (Cloutier et al., 2015), MSCI does not kill spermatocytes, and asynaptic oocytes are not eliminated in a pattern typical of DNA repair mutants.

The pachytene checkpoint has commonly been thought to consist of separate DNA damage and synapsis checkpoints in multiple organisms. However, the finding that MSUC can cause the death of oocytes led to the suggestion that there is only 1 formal cell cycle checkpoint in mouse oocytes, the DNA damage checkpoint (Cloutier et al., 2015), - and our data provide mechanistic evidence consistent with this idea. Current information supports a model (Figure 6D) for two major mechanisms by which oocytes with synapsis defects are eliminated: 1) MSUC, for oocytes with a small number of asynapsed chromosomes that do not accumulate unrepaired DSBs above a threshold and in which both homologs bear essential genes for meiotic progression are silenced (Cloutier et al., 2015), and the DNA damage checkpoint, for oocytes with multiple asynapsed chromosomes that accumulate a sufficient number of DSBs to trigger the DNA damage checkpoint (Figure 6D). These disparate mechanisms may have distinct purposes. Because oocytes with only 1 or 2 unsynapsed chromosomes may not efficiently trigger the spindle assembly checkpoint (SAC) (LeMaire-Adkins et al., 1997), the MSUC pathway would safeguard against aneuploidy. Superficially, it would seem that, because oocytes with extensive asynapsis would effectively trigger the SAC, the DNA damage checkpoint mechanism is redundant. However, it is likely advantageous reproductively to eliminate such defective oocytes before they enter dictyate as constituents of the ovarian reserve, otherwise the fraction of unproductive ovulations (those terminated by the SAC) would increase, compromising fecundity.

STAR★METHODS

Detailed methods are provided in the online version of this paper and include the following:

- KEY RESOURCES TABLE
- CONTACT FOR REAGENT AND RESOURCE SHARING
- EXPERIMENTAL MODEL AND SUBJECT DETAILS
- METHOD DETAILS
  - Organ Culture and Irradiation
  - Histology and Immunostaining
  - Immunofluorescence of meiotic chromosome surface spreads
  - Focus Quantification
  - Fertility Test
- QUANTIFICATION AND STATISTICAL ANALYSIS
  - Statistical analysis
- DATA AND SOFTWARE AVAILABILITY

SUPPLEMENTAL INFORMATION

Supplemental Information includes five figures and three tables and can be found with this article online at http://dx.doi.org/10.1016/j.molcel.2017.07.027.

AUTHOR CONTRIBUTIONS

V.D.R. and E.B.F. performed the experiments and contributed to the writing of the paper. H Kogo and H. Kurahashi provided the *Hormad2* mutant ESCs and provided feedback on the manuscript. J.C.S. supervised the work and wrote most of the paper.

ACKNOWLEDGMENTS

This work was supported by a grant from the NIH (R01 GM45415 to J.C.S.) and contract CO29155 from the New York State Stem Cell Program (NYSTEM). The authors would like to thank R. Munroe and C. Abratte for generating chimeric mice, Stephen Parry from the Cornell Statistical Consulting Unit for help with statistical analysis, Dr. Atilla Toth for the HORMAD2 antibody, and M.A. Handel for feedback on the manuscript.

Received: April 3, 2017
Revised: June 14, 2017
Accepted: July 28, 2017
Published: August 24, 2017

REFERENCES

Agoulnik, A.I., Lu, B., Zhu, Q., Truong, C., Ty, M.T., Arango, N., Chada, K.K., and Bishop, C.E. (2002). A novel gene, *Pog*, is necessary for primordial germ cell proliferation in the mouse and underlies the germ cell deficient mutation, gcd. Hum. Mol. Genet. *11*, 3047–3053.

Baudat, F., Manova, K., Yuen, J.P., Jasin, M., and Keeney, S. (2000). Chromosome synapsis defects and sexually dimorphic meiotic progression in mice lacking *Spo11*. Mol. Cell *6*, 989–998.

Bellani, M.A., Romanienko, P.J., Cairatti, D.A., and Camerini-Otero, R.D. (2005). SPO11 is required for sex-body formation, and *Spo11* heterozygosity rescues the prophase arrest of *Atm*-/- spermatocytes. J. Cell Sci. *118*, 3233–3245.

Bolcun-Filas, E., Rinaldi, V.D., White, M.E., and Schimenti, J.C. (2014). Reversal of female infertility by Chk2 ablation reveals the oocyte DNA damage checkpoint pathway. Science *343*, 533–536.

Burgoyne, P.S., and Baker, T.G. (1985). Perinatal oocyte loss in XO mice and its implications for the aetiology of gonadal dysgenesis in XO women. J. Reprod. Fertil. *75*, 633–645.

Carballo, J.A., Johnson, A.L., Sedgwick, S.G., and Cha, R.S. (2008). Phosphorylation of the axial element protein Hop1 by Mec1/Tel1 ensures meiotic interhomolog recombination. Cell *132*, 758–770.

Carofiglio, F., Inagaki, A., de Vries, S., Wassenaar, E., Schoenmakers, S., Vermeulen, C., van Cappellen, W.A., Sleddens-Linkels, E., Grootegoed, J.A., Te Riele, H.P., et al. (2013). SPO11-independent DNA repair foci and their role in meiotic silencing. PLoS Genet. *9*, e1003538.

Cloutier, J.M., Mahadevaiah, S.K., Ellnati, E., Nussenzweig, A., Tóth, A., and Turner, J.M. (2015). Histone H2AFX links meiotic chromosome asynapsis to prophase I oocyte loss in mammals. PLoS Genet. *11*, e1005462.

Conrad, D.F., Keebler, J.E., DePristo, M.A., Lindsay, S.J., Zhang, Y., Casals, F., Idaghdour, Y., Hartl, C.L., Torroja, C., Garimella, K.V., et al.; 1000 Genomes Project (2011). Variation in genome-wide mutation rates within and between human families. Nat. Genet. *43*, 712–714.

Daniel, K., Lange, J., Hached, K., Fu, J., Anastassiadis, K., Roig, I., Cooke, H.J., Stewart, A.F., Wassmann, K., Jasin, M., et al. (2011). Meiotic homologue alignment and its quality surveillance are controlled by mouse HORMAD1. Nat. Cell Biol. *13*, 599–610.

Di Giacomo, M., Barchi, M., Baudat, F., Edelmann, W., Keeney, S., and Jasin, M. (2005). Distinct DNA-damage-dependent and -independent responses drive the loss of oocytes in recombination-defective mouse mutants. Proc. Natl. Acad. Sci. USA *102*, 737–742.

Fernandez-Capetillo, O., Celeste, A., and Nussenzweig, A. (2003). Focusing on foci: H2AX and the recruitment of DNA-damage response factors. Cell Cycle *2*, 426–427.

Finsterbusch, F., Ravindranathan, R., Dereli, I., Stanzione, M., Tränkner, D., and Tóth, A. (2016). Alignment of homologous chromosomes and effective repair of programmed DNA double-strand breaks during mouse meiosis require the minichromosome maintenance domain containing 2 (MCMDC2) protein. PLoS Genet. *12*, e1006393.

Goldfarb, T., and Lichten, M. (2010). Frequent and efficient use of the sister chromatid for DNA double-strand break repair during budding yeast meiosis. PLoS Biol. *8*, e1000520.

Gray, S., and Cohen, P.E. (2016). Control of meiotic crossovers: from double-strand break formation to designation. Annu. Rev. Genet. *50*, 175–210.

Hirao, A., Cheung, A., Duncan, G., Girard, P.M., Elia, A.J., Wakeham, A., Okada, H., Sarkissian, T., Wong, J.A., Sakai, T., et al. (2002). Chk2 is a tumor suppressor that regulates apoptosis in both an ataxia telangiectasia mutated (ATM)-dependent and an ATM-independent manner. Mol. Cell. Biol. *22*, 6521–6532.

Homolka, D., Jansa, P., and Forejt, J. (2012). Genetically enhanced asynapsis of autosomal chromatin promotes transcriptional dysregulation and meiotic failure. Chromosoma *121*, 91–104.

Ichijima, Y., Ichijima, M., Lou, Z., Nussenzweig, A., Camerini-Otero, R.D., Chen, J., Andreassen, P.R., and Namekawa, S.H. (2011). MDC1 directs chromosome-wide silencing of the sex chromosomes in male germ cells. Genes Dev. *25*, 959–971.

Joshi, N., Brown, M.S., Bishop, D.K., and Börner, G.V. (2015). Gradual implementation of the meiotic recombination program via checkpoint pathways controlled by global DSB levels. Mol. Cell *57*, 797–811.

Kauppi, L., Barchi, M., Lange, J., Baudat, F., Jasin, M., and Keeney, S. (2013). Numerical constraints and feedback control of double-strand breaks in mouse meiosis. Genes Dev. *27*, 873–886.

Kogo, H., Tsutsumi, M., Inagaki, H., Ohye, T., Kiyonari, H., and Kurahashi, H. (2012a). HORMAD2 is essential for synapsis surveillance during meiotic prophase via the recruitment of ATR activity. Genes Cells *17*, 897–912.

Kogo, H., Tsutsumi, M., Ohye, T., Inagaki, H., Abe, T., and Kurahashi, H. (2012b). HORMAD1-dependent checkpoint/surveillance mechanism eliminates asynaptic oocytes. Genes Cells *17*, 439–454.

Kouznetsova, A., Wang, H., Bellani, M., Camerini-Otero, R.D., Jessberger, R., and Höög, C. (2009). BRCA1-mediated chromatin silencing is limited to oocytes with a small number of asynapsed chromosomes. J. Cell Sci. *122*, 2446–2452.

Lam, I., and Keeney, S. (2014). Mechanism and regulation of meiotic recombination initiation. Cold Spring Harb. Perspect. Biol. *7*, a016634.

Latypov, V., Rothenberg, M., Lorenz, A., Octobre, G., Csutak, O., Lehmann, E., Loidl, J., and Kohli, J. (2010). Roles of Hop1 and Mek1 in meiotic chromosome pairing and recombination partner choice in *Schizosaccharomyces pombe*. Mol. Cell. Biol. *30*, 1570–1581.

LeMaire-Adkins, R., Radke, K., and Hunt, P.A. (1997). Lack of checkpoint control at the metaphase/anaphase transition: a mechanism of meiotic nondisjunction in mammalian females. J. Cell Biol. *139*, 1611–1619.

Li, X.C., and Schimenti, J.C. (2007). Mouse pachytene checkpoint 2 (*trip13*) is required for completing meiotic recombination but not synapsis. PLoS Genet. *3*, e130.

Li, X.C., Bolcun-Filas, E., and Schimenti, J.C. (2011). Genetic evidence that synaptonemal complex axial elements govern recombination pathway choice in mice. Genetics *189*, 71–82.

Luo, Y., Hartford, S.A., Zeng, R., Southard, T.L., Shima, N., and Schimenti, J.C. (2014). Hypersensitivity of primordial germ cells to compromised replication-associated DNA repair involves ATM-p53-p21 signaling. PLoS Genet. *10*, e1004471.

MacQueen, A.J., and Hochwagen, A. (2011). Checkpoint mechanisms: the puppet masters of meiotic prophase. Trends Cell Biol. *21*, 393–400.

Malki, S., van der Heijden, G.W., O'Donnell, K.A., Martin, S.L., and Bortvin, A. (2014). A role for retrotransposon LINE-1 in fetal oocyte attrition in mice. Dev. Cell *29*, 521–533.

Maltaris, T., Seufert, R., Fischl, F., Schaffrath, M., Pollow, K., Koelbl, H., and Dittrich, R. (2007). The effect of cancer treatment on female fertility and strategies for preserving fertility. Eur. J. Obstet. Gynecol. Reprod. Biol. *130*, 148–155.

Mao-Draayer, Y., Galbraith, A.M., Pittman, D.L., Cool, M., and Malone, R.E. (1996). Analysis of meiotic recombination pathways in the yeast Saccharomyces cerevisiae. Genetics *144*, 71–86.

Meirow, D., and Nugent, D. (2001). The effects of radiotherapy and chemotherapy on female reproduction. Hum. Reprod. Update *7*, 535–543.

Murphey, P., McLean, D.J., McMahan, C.A., Walter, C.A., and McCarrey, J.R. (2013). Enhanced genetic integrity in mouse germ cells. Biol. Reprod. *88*, 6.

Nadler, J.J., and Braun, R.E. (2000). Fanconi anemia complementation group C is required for proliferation of murine primordial germ cells. Genesis *27*, 117–123.

Niu, H., Wan, L., Baumgartner, B., Schaefer, D., Loidl, J., and Hollingsworth, N.M. (2005). Partner choice during meiosis is regulated by Hop1-promoted dimerization of Mek1. Mol. Biol. Cell *16*, 5804–5818.

Pacheco, S., Marcet-Ortega, M., Lange, J., Jasin, M., Keeney, S., and Roig, I. (2015). The ATM signaling cascade promotes recombination-dependent pachytene arrest in mouse spermatocytes. PLoS Genet. *11*, e1005017.

Perez, G.I., Knudson, C.M., Leykin, L., Korsmeyer, S.J., and Tilly, J.L. (1997). Apoptosis-associated signaling pathways are required for chemotherapy-mediated female germ cell destruction. Nat. Med. *3*, 1228–1232.

Peters, A.H., Plug, A.W., van Vugt, M.J., and de Boer, P. (1997). A drying-down technique for the spreading of mammalian meiocytes from the male and female germline. Chromosome Res. *5*, 66–68.

Pittman, D.L., Cobb, J., Schimenti, K.J., Wilson, L.A., Cooper, D.M., Brignull, E., Handel, M.A., and Schimenti, J.C. (1998). Meiotic prophase arrest with failure of chromosome synapsis in mice deficient for Dmc1, a germline-specific RecA homolog. Mol. Cell *1*, 697–705.

Reinholdt, L.G., and Schimenti, J.C. (2005). *Mei1* is epistatic to *Dmc1* during mouse meiosis. Chromosoma *114*, 127–134.

Reinholdt, L., Ashley, T., Schimenti, J., and Shima, N. (2004). Forward genetic screens for meiotic and mitotic recombination-defective mutants in mice. Methods Mol. Biol. *262*, 87–107.

Rinaldi, V.D., Hsieh, K., Munroe, R., Bolcun-Filas, E.M., and Schimenti, J.C. (2017). Pharmacological inhibition of the DNA damage checkpoint prevents radiation-induced oocyte death. Genetics. Published online June 2, 2017. http://dx.doi.org/10.1534/genetics.117.203455.

Roeder, G.S., and Bailis, J.M. (2000). The pachytene checkpoint. Trends Genet. *16*, 395–403.

Schindelin, J., Arganda-Carreras, I., Frise, E., Kaynig, V., Longair, M., Pietzsch, T., Preibisch, S., Rueden, C., Saalfeld, S., Schmid, B., et al. (2012). Fiji: an open-source platform for biological-image analysis. Nat. Methods *9*, 676–682.

Schwacha, A., and Kleckner, N. (1997). Interhomolog bias during meiotic recombination: meiotic functions promote a highly differentiated interhomolog-only pathway. Cell *90*, 1123–1135.

Shin, Y.H., Choi, Y., Erdin, S.U., Yatsenko, S.A., Kloc, M., Yang, F., Wang, P.J., Meistrich, M.L., and Rajkovic, A. (2010). *Hormad1* mutation disrupts synaptonemal complex formation, recombination, and chromosome segregation in mammalian meiosis. PLoS Genet. *6*, e1001190.

Shin, Y.H., McGuire, M.M., and Rajkovic, A. (2013). Mouse HORMAD1 is a meiosis i checkpoint protein that modulates DNA double- strand break repair during female meiosis. Biol. Reprod. *89*, 29.

Smith, J., Tho, L.M., Xu, N., and Gillespie, D.A. (2010). The ATM-Chk2 and ATR-Chk1 pathways in DNA damage signaling and cancer. Adv. Cancer Res. *108*, 73–112.

Stambrook, P.J., and Tichy, E.D. (2010). Preservation of genomic integrity in mouse embryonic stem cells. Adv. Exp. Med. Biol. *695*, 59–75.

Stanzione, M., Baumann, M., Papanikos, F., Dereli, I., Lange, J., Ramlal, A., Tränkner, D., Shibuya, H., de Massy, B., Watanabe, Y., et al. (2016). Meiotic DNA break formation requires the unsynapsed chromosome axis-binding protein IHO1 (CCDC36) in mice. Nat. Cell Biol. *18*, 1208–1220.

Subramanian, V.V., and Hochwagen, A. (2014). The meiotic checkpoint network: step-by-step through meiotic prophase. Cold Spring Harb. Perspect. Biol. *6*, a016675.

Subramanian, V.V., MacQueen, A.J., Vader, G., Shinohara, M., Sanchez, A., Borde, V., Shinohara, A., and Hochwagen, A. (2016). Chromosome synapsis alleviates Mek1-dependent suppression of meiotic DNA repair. PLoS Biol. *14*, e1002369.

Suh, E.K., Yang, A., Kettenbach, A., Bamberger, C., Michaelis, A.H., Zhu, Z., Elvin, J.A., Bronson, R.T., Crum, C.P., and McKeon, F. (2006). p63 protects the female germ line during meiotic arrest. Nature *444*, 624–628.

Turner, J.M., Aprelikova, O., Xu, X., Wang, R., Kim, S., Chandramouli, G.V., Barrett, J.C., Burgoyne, P.S., and Deng, C.X. (2004). BRCA1, histone H2AX phosphorylation, and male meiotic sex chromosome inactivation. Curr. Biol. *14*, 2135–2142.

van der Heijden, G.W., and Bortvin, A. (2009). Transient relaxation of transposon silencing at the onset of mammalian meiosis. Epigenetics *4*, 76–79.

Watanabe, N., Mii, S., Asai, N., Asai, M., Niimi, K., Ushida, K., Kato, T., Enomoto, A., Ishii, H., Takahashi, M., and Murakumo, Y. (2013). The REV7 subunit of DNA polymerase ζ is essential for primordial germ cell maintenance in the mouse. J. Biol. Chem. *288*, 10459–10471.

Wojtasz, L., Daniel, K., Roig, I., Bolcun-Filas, E., Xu, H., Boonsanay, V., Eckmann, C.R., Cooke, H.J., Jasin, M., Keeney, S., et al. (2009). Mouse HORMAD1 and HORMAD2, two conserved meiotic chromosomal proteins, are depleted from synapsed chromosome axes with the help of TRIP13 AAA-ATPase. PLoS Genet. *5*, e1000702.

Wojtasz, L., Cloutier, J.M., Baumann, M., Daniel, K., Varga, J., Fu, J., Anastassiadis, K., Stewart, A.F., Reményi, A., Turner, J.M., and Tóth, A. (2012). Meiotic DNA double-strand breaks and chromosome asynapsis in mice are monitored by distinct HORMAD2-independent and -dependent mechanisms. Genes Dev. *26*, 958–973.

STAR★METHODS

KEY RESOURCES TABLE

REAGENT or RESOURCE	SOURCE	IDENTIFIER
Antibodies		
mouse anti-p63	Novus Biologicals	Novus Cat# NB 100-691; RRID: AB_525968
rabbit anti-MVH	Abcam	Abcam Cat# ab13840; RRID: AB_443012
rabbit anti-RAD51 Chip-Grade	Abcam	Abcam Cat# ab176458; RRID: AB_2665405
mouse anti-SYCP3	Abcam	Abcam Cat# ab97672; RRID: AB_10678841
guinea pig anti-HORMAD2	Wojtasz et al., 2012	gift from Dr. Attila Toth
Deposited Data		
Raw images	This paper; Mendeley Data	http://dx.doi.org/10.17632/3n2yfpk4vh.1
Experimental Models: Organisms/Strains		
Mouse: *Trip13*$^{Gt/Gt}$: *Trip13*$^{Gt(RRB047)Byg}$	Li and Schimenti, 2007	RRID:MGI:372059
Mouse: *Dmc1*$^{-/-}$: *Dmc1*^{tm1Jcs}	Pittman et al., 1998	RRID:MGI:3768914
Mouse: *Chk2*$^{-/-}$: *Chk2*^{tm1Mak}	Tak Mak; Hirao et al., 2002	RRID:MGI:2662578
Mouse: *Spo11*$^{-/-}$: *Spo11*^{tm1Mjn}	Maria Jasin; Baudat et al., 2000	RRID:MGI:4358251
Mouse: *Hormad2*$^{-/-}$: *Hormad2*	Kogo et al., 2012a	RRID:MGI:5466572
Software and Algorithms		
JMP Pro12 software v.12.0.1	SAS Inc., Cary, NC-USA	RRID:SCR_014242
Fiji-ImageJ	Schindelin et al., 2012	RRID:SCR_002285

CONTACT FOR REAGENT AND RESOURCE SHARING

Further information and requests for reagents may be directed to and will be fulfilled by the Lead Contact, John Schimenti (jcs92@cornell.edu).

EXPERIMENTAL MODEL AND SUBJECT DETAILS

Experiments were performed on female mice, and of course male mice were used for matings to produce desired genotypes. Samples for histological analysis were from eight week old animals. The alleles used have been previously described and were the following: *Trip13*$^{Gt(RRB047)Byg}$ (referred to as *Trip13*^{Gt} in the manuscript) (Li and Schimenti, 2007); *Dmc1*^{tm1Jcs} (Pittman et al., 1998); *Chk2*^{tm1Mak} (Hirao et al., 2002); *Spo11*^{tm1Mjn} (Baudat et al., 2000); and *Hormad2* (Kogo et al., 2012a). All mice were in a mixed genetic background of strains C57BL/6J and C3H/HeJ. The Cornell's Animal Care and Use Committee approved all animal usage, under protocol 2004-0038 to JCS.

The embryonic age of pre-term animals was counted using the morning in which copulation plug was detected as being the 0.5 days post coitus (dpc).

METHOD DETAILS

Organ Culture and Irradiation

Embryonic and pp explanted ovaries were cultured under conditions as we previously detailed (Rinaldi et al., 2017). Ovaries were irradiated in a ^{137}cesium irradiator with a rotating turntable. Immediately after irradiation, the media was replaced, and ovaries were cultured for indicated periods of time prior to tissue processing.

Histology and Immunostaining

Ovaries were dissected and incubated in Bouin's fixative overnight at room temperature. Afterward, tissues were washed in 70% ethanol prior to being embedded in paraffin for serial sectioning at 6 μm thickness. Ovaries were stained with Harris Hematoxylin and Eosin (H&E) and follicles counted in every fifth section except for the three-week counts reported in Figure 1B, in which every 12th section was counted. There was no correction factor applied to the values reported. Only one ovary per animal was used.

Cultured ovaries, used for histological sections followed by immunostaining, were fixed in 4% paraformaldehyde/PBS over night at 4°C. After 70% ethanol washes, ovaries were embedded in paraffin and serially sectioned at 5 μm. These ovaries were immunostained using standard methods. Briefly, slides were deparaffinized and re-hydrated prior to antigen retrieval using sodium citrate buffer. Slides were blocked with 5% goat serum (PBS/Tween 20) and incubated at 4°C overnight with primary antibodies: mouse anti-p63 (1:500, 4A4, Novus Biologicals); and rabbit anti-MVH (1:1000, Abcam). Afterward, sections were incubated with Alexa Fluor® secondary antibodies for one hour and Hoechst dye for 5 min. Slides were mounted with ProLong Anti-fade (Thermo-Fisher) and imaged.

Histological images were obtained from slides digitized using a Leica Scanscope CS2.

Immunofluorescence of meiotic chromosome surface spreads

Meiotic surface spreads of prophase I female meiocytes were prepared using an adaptation (Reinholdt et al., 2004) of a drying-down technique (Peters et al., 1997) that was described in great detail in the former reference. Meiotic stages (leptonema-diakinesis) were determined based on SYCP3 staining patterns (Gray and Cohen, 2016). Slides were stored at −80°C until immunostained. For staining, slides were brought to room temperature (RT) and washed once with PBS+0.1% Tween-20 (PBS-T). Slides were blocked for 40 min at RT with PBS-T containing 5% normal goat serum (5%GS-PBS-T). Primary antibodies were diluted into 5%GS-PBS-T and incubated overnight at RT in a humidified chamber. Antibodies and dilutions used included: rabbit anti-RAD51 (1:250 Abcam 176458), mouse anti-SYCP3 (1:600 Abcam) and guinea pig anti-HORMAD2 antibody (1:1000, kind gift from Attila Toth). Secondary antibodies used were diluted 1:1000 in in 5%GS-PBS-T and included goat anti-rabbit Alexa 488/594, goat anti-mouse Alexa 488/594 and goat anti-guinea pig Alexa 488/594. Images were taken using an Olympus microscope with 40X lens or 100X immersion oil lens and CCD camera.

Focus Quantification

Foci were quantified both manually, through the visualization and annotation of individual foci, and also semi-automatically using Fiji-ImageJ (Schindelin et al., 2012). Semi-automated counts were performed using binary images obtained from the RAD51-labeled channel, with the threshold set above background level. The count was obtained after performing "Watershed," by the "Analyze Particles" functionality with size set for 1.5 to infinity. Cell counts that displayed discrepancy of more than 20% between manual and semi-automated counts were discarded.

Fertility Test

To test if HORMAD2 deficiency was able to rescue the *Trip13*$^{Gt/Gt}$ sterility phenotype, three double mutant females were mated to WT C3H/HeJ males proven to be fertile through previous matings. Each female provided more than 4 consecutive litters up to the time of preparation of this manuscript. All three females originated from different litters. *Trip13*$^{Gt/Gt}$ littermates were housed with fertile males and used as negative controls.

QUANTIFICATION AND STATISTICAL ANALYSIS

Statistical analysis

Comparisons between compound mutants and controls were done using littermates or related animals. Unless otherwise noted, all experiments used at least three mice per experimental group. All statistical analyses were done using JMP Pro12 software (SAS Inc., Cary, NC-USA, version 12.0.1). Comparisons of fertility and follicle counts between genotypic groups were tested using both the Tukey honest significance different (HSD) and the non-parametric, one-way ANOVA test (Kruskal -Wallis). Both tests provided concordant results. RAD51 focus counts were analyzed using a mixed model with animal ID as random effect and genotype as fixed effect. Least square means (LSMeans) differences were tested using Tukey HSD. The residuals from the mixed model were normally distributed.

DATA AND SOFTWARE AVAILABILITY

Raw data of RAD51 foci counts are in supplementary tables (Table S1, Table S2, and Table S3). The raw image files can be downloaded at Mendeley data: http://dx.doi.org/10.17632/3n2yfpk4vh.1.